



A PVD Joining Hybrid Process for Manufacturing Complex Metal Composites

A unique brazing method offers the possibilities of joining very small and geometrically diverse components

BY FR.-W. BACH, T. A. DEISSER, U. HOLLAENDER, K. MOEHWALD, AND M. NICOLAUS

ABSTRACT. In the present work, a new hybrid process is introduced: the gas/solid-transient liquid phase (TLP) bonding. With this process, the filler metal is transported by a gaseous phase to the joining area. The filler metal reacts with the base metal by a metallurgical gas-solid reaction and forms a liquid transition phase, which solidifies isothermally during further heat treatment. In this work, a fundamental investigation was made of the process, and simple model systems such as antimony (gas.)/iron (sol.), antimony (gas.)/steel (sol.), and zinc (gas.)/nickel (sol.) were developed. The entire process was modeled, taking into account the physical sequences (filler metal evaporating, filler metal transport to the joining areas, filler metal adsorption to the base metal, alloying of the filler metal and the base metal, isothermal solidification). The gas/solid-TLP-bonding process allows the joining of very small and complex components, where up to now no suitable joining process existed.

Introduction

For manufacturing complex metal components, soldering or brazing is often the sole way of realizing tight and strong joints between the manufacturing materials. The choice of the filler metal depends on the base material, the brazed joint requirements, and the brazing technique (Refs. 1, 2). The application of the filler metal is usually effected in the form of wires, foils, pastes, and increasingly by coatings like PVD, CVD, electroless and electrodeposited layers, as well as thermal spraying (Refs. 3–9).

Especially with the application of PVD technology, further development of the brazing with isothermal solidification oc-

curred using transient-liquid-phase (TLP) bonding (Refs. 10–12). This technology is characterized by the use of heterogeneous solder systems, which show a low melting eutectic on their own or in combination with the base material. During the brazing process, a eutectic liquid transient phase is constituted at the surfaces of the base material, which again solidifies with further heat treatment and develops a strong and tight joint.

For joining very small and geometrical ambitious components, the filler metal dosage has to be very accurate. With further miniaturization of the joining components, coating technologies reach their limits with brazing, considering the complex handling required (i.e., positioning of the components in a PVD-recipient or in an electrolyte solution for electro- or electroless deposition). Due to these facts, it is desirable to develop a new joining technology that applies the filler metal in a different way than the standard brazing process; for example, transporting the filler metal to the base materials through a gaseous phase during brazing. Subsequently, a metallurgical gas/solid reaction occurs and a liquid transition phase is constituted, which solidifies during further heat treatment. This is the so-called gas/solid-TLP-bonding process.

The principle of the gas/solid-TLP bonding can be divided into five sequences. In the first stage, the filler metal evaporates in an evacuated container.

During the second stage, the gaseous filler metal is transported to the surface of the specimens by means of convective gas flow. The third stage describes the adsorption of the filler metal onto the specimen's surface. Accordingly, in stage 4, the alloying of the filler metal with components from the base material proceeds until the formation of a liquid transition phase takes place. Finally, in stage five, there is an isothermal solidification of the alloy by means of further enrichment of the components from the base material caused by diffusion processes.

For a successful joining process, some conditions have to be met. There must be suitable kinetics. That means that the transport of the filler metal onto the specimen's surface has to be faster than the alloying of the filler metal with the base material to the solid composition, because otherwise no transient liquid phase is formed. Hence, the vapor pressure of the solder metal has to be sufficiently high to be transported to the specimens. Lastly, suitable mixing thermodynamics must be taken into account, since a liquid solder-poor alloy has to exist within the filler metal/base material system at the dedicated temperature.

This leads to an appropriate model system: the iron-antimony system — Fig. 1. This system was chosen because it is of practical relevance; the filler metal, as mentioned above, has to be transported by means of a convective gas flow onto the specimen's surface. The properties for antimony (vapor pressure of 35 mbar at 1100°C [Ref. 13]) are given. Finally, at this temperature, antimony can be alloyed to iron with a substance of 0.7 before reaching the solidus of α -iron.

The gray line and the right axis of the phase diagram represent the thermodynamic activity of antimony in an idealized form, according to Raoult's law.

Alloying on the iron surface takes place with antimony, and the Sb-activity

KEYWORDS

Brazing
Filler Metal
Gas/Solid Reaction
Liquid Transition
Soldering
Vapor

FR.-W. BACH, T. A. DEISSER, U. HOLLAENDER, K. MOEHWALD, and M. NICOLAUS are with the Institute of Materials Science, Leibniz University of Hanover, Germany.

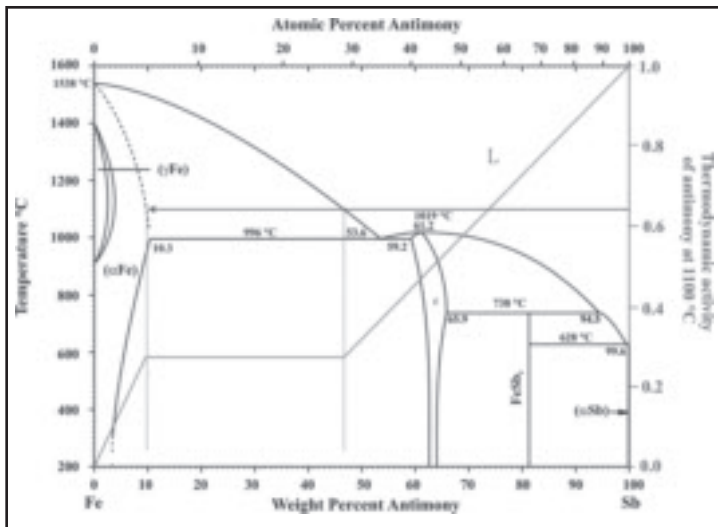


Fig. 1 — Phase diagram of Fe-Sb.

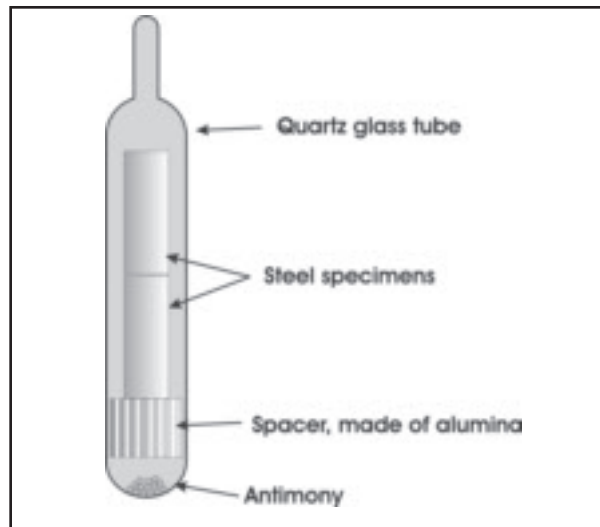


Fig. 2 — Process cell.

decreases by reason of vapor pressure degradation over the mixture. Concerning the activity varieties of antimony, a Sb-transport is initiated (thermodynamic power). By a further diffusion process (Sb diffuses into Fe and/or vice versa), an alloying up to α -Fe proceeds and an isothermal solidification occurs that is characteristic for the TLP bonding (Refs. 14, 15).

$$a_{Sb}(T, x_{Sb}) = \frac{p_{Sb}(T, x_{Sb})}{p_{Sb}^0(T)}$$

$$\text{with } \lim_{x_{Sb} \rightarrow 1} a_{Sb} = 1 \left(\begin{array}{l} \text{Raoult's} \\ \text{standardization} \end{array} \right) \quad (1)$$

Where $a_{Sb}(T, x_{Sb})$ = Sb activity

$p_{Sb}(T, x_{Sb})$ = Sb-vapor pressure over the mixture

$p_{Sb}^0(T)$ = vapor pressure of pure Sb at temperature T

Experimental

Brazing experiments were carried out in a process cell made of quartz-glass — Fig. 2. At the bottom of the cell, antimony granules were deposited in an amount of about 100 mg. A spacer made of alumina or quartz glass was located slightly above to separate the iron specimens from the antimony. The iron rods were 20 mm long and 8 mm in diameter, and were placed onto the spacer. The front surfaces of the rods were face ground in such a way that a maximum joint clearance of 20 microns was in between. The prepared process cell was connected to a rotary vane pump, evacuated (approximately 10^{-3} mbar), melted off, and placed in a furnace for further heat treatment. The process times varied from 2.5 h up to 10 h, and all ex-

periments were carried out at a temperature of 1100°C. For microstructure investigations, the brazed specimens were cut through, ground, polished, and micrographs were made.

Results

Figure 3 shows the cross sections of the samples brazed for 2.5–10 h at 1100°C. For the sample processed for 2.5 h at 1100°C, a partial closed brazing joint clearance (approximately 70 μm) was observed. The bright phase within the brazing clearance was identified as ϵ phase (FeSb). With the sample for the 5-h process, the joint clearance was just 20 μm wide, and it was nearly closed after 7.5 h, showing the ϵ phase just in some isolated areas. Complete filling was reached after 10 h. This behavior is reasonable with the diffusion process. The longer the heat treatment, the more antimony was able to diffuse into the iron (and contrary) until the solidus of α -Fe was reached. Figure 4 depicts a cross section of a brazed steel sample. Except for a few pores within the contact area, the joint clearance was entirely filled. Despite etching, no differing phases from the base material were found. The specimen was a homogenous compact body. However, SEM-studies revealed a Fe-Sb-mixed phase at the border area (ϵ phase of the Fe-Sb-phase diagram).

On the other hand, inside the body, the brazed joint, by reason of the long heat treatment, was alloyed such that no more ϵ phase was detected. The braze joint was a compact single-phased area of α iron, containing less than 2 at.-% of Sb. This sample was “welded” far below its melting temperature.

Butt joint round specimens, brazed with gaseous antimony and provided with exter-

nal screw threads for fixing, were tensile tested. The metallographic results were reflected by the tensile strength data outlined in Fig. 6. As the heat treatment period increased and an accordingly decrease in Fe-Sb phases within the braze joint occurred, the tensile strength grew to a final value of 177 MPa after 10 h — Figs. 5, 6.

Discussion

The sequences of this new joining technique are structured as follows:

- 1) Filler metal evaporation inside a vacuum chamber
- 2) Filler metal transport to the brazing joint by convective gas flow
- 3) Filler metal adsorption onto the base material surface
- 4) Alloying with constituents from the base material to form a liquid alloy film within the braze joint
- 5) Isothermal alloy solidification within the braze joint by further enrichment with constituents from the base material.

Antimony Transport over Gaseous Phase by Convective Gas Flow

Steps 1 and 2 — Proceeding on the assumption of freely exposed surfaces, the material transport in the gaseous phase of sequences 1 and 2 proceeds so fast that these steps do not affect the total kinetics, e.g., between solid iron and gaseous antimony. The vapor pressure is the equilibrium vapor pressure of the pure filler metal, as a function of temperature. However, thin gaps indicate a reduced vapor pressure, because the alloying occurring reduces the thermodynamic activity of antimony. At first approximation, the vapor pressure within small cavities can be at-

tributed to Raoult's law. The resulting pressure deviation between the inner gap and the free ambient gas affects the convective gas transport in the cavity. Furthermore, this depends on the inlet geometry. So, additionally, the inlet geometry must be taken into account, the dimensions of which constitute the free path of the gaseous particles, and the gas transport must be regarded as a Knudsen-effusion. Reaction conditions existing with the antimony experiments (750°C up to 1100°C) resulted in vapor pressures of approximately 3000 Pa maximum — Fig. 4. Consequently, transport within the gaseous phase can be described in good approximation, according to ideal gases.

Adsorption of Sb onto the Fe-Surface

Step 3 — For describing the adsorption occurrences at the border of the solid/gaseous phase, a set of rules for the characterization of such adsorption isotherms exist. On one hand experimental data is required. On the other hand, known appendages about diffusion processes into the solid, as well as chemical reactions between gaseous and solid phase, must be considered. In the case of gaseous antimony, which adsorbs on solid iron, an immediate alloying up to the liquidus curve will occur, causing a reduction of the thermodynamic activity of the adsorbing gaseous Sb in comparison with the ambient gaseous Sb. On this basis — beyond the knowledge of precise adsorption isotherms — the maximum possible adsorption rate can be formulated as the number of collisions per time unit of antimony atoms on the interface (less the desorbed Sb atoms at reduced vapor pressure). This leads to a simplified dependency of the mass-oriented Sb-adsorption rate on the temperature and composition of the formed alloy layer at the liquidus curve

$$\frac{m_{Sb-adsorbed}}{A} = (p_{Sb} - X_{Sb-Liquidus} p_{Sb}^0) \sqrt{\frac{2\pi M_{Sb}}{RT}} \quad (2)$$

where $\frac{m_{Sb-adsorbed}}{A}$ = mass-oriented adsorption rate per Area A

$X_{Sb-Liquidus}$ = amount of substance Sb at liquidus (dependent on T, cp. Fig. 1)

M_{Sb} = molar mass Sb

p_{Sb} = vapor pressure Sb above surface

p_{Sb}^0 = vapor pressure equilibrium of pure Sb

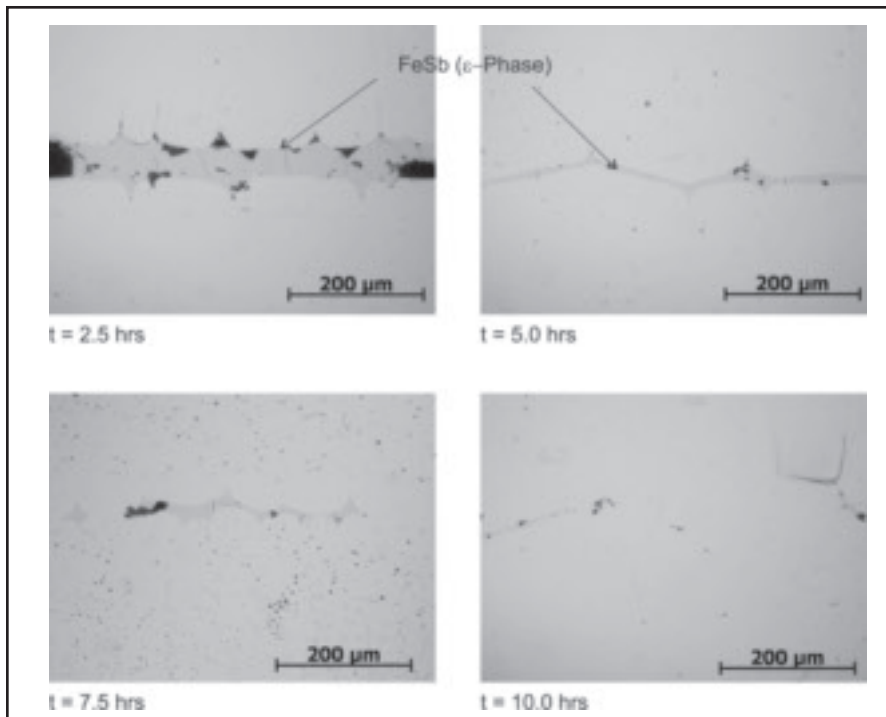


Fig. 3 — Cross sections of brazed specimens.

Diffusion Processes at the Fe-Sb System

Steps 4 and 5 — Basic principle for describing the diffusion process is the following equation (Fick's 2nd law):

$$\frac{\partial c}{\partial t} = D \cdot \frac{\partial^2 c}{\partial x^2} \quad (3)$$

where c = concentration (particle density), t = time, x = location coordinate, and D = diffusion coefficient.

If the diffusion coefficient D is not a function of the particle density N and the location x , then Equation 3 is valid. From the presented experiments and the test conditions, the results indicate the following method of resolution:

Figure 8 shows the braze experiment sequence. First, the joint clearance d_0 between the iron samples is closed by means of gaseous phase transported antimony. Iron is alloyed. Until the liquidus equilibrium is reached, iron is alloyed by antimony because of occurring diffusion processes (Sb diffuses into Fe and vice versa). At 1100°C, $c_{Sb(liq.)} = 47$ wt-% — Fig. 1. Due to the formed liquid phase, d_0 expands to the area $d_{liq.}$, where an iron-antimony mixture is located. Having the formation of a liquid transient phase, antimony diffuses further into the iron substrate. The Fe-Sb phase is impoverished of antimony until the isothermal solidification is initiated. The solidus equi-

librium concentration is reached. At 1100°C $c_{Sb(sol.)}$ amounts to 10 wt-%.

The change in joint clearance width is given from

$$\begin{aligned} d_{liq.} &= \frac{1}{A} \cdot n_{Sb} \cdot \bar{V}_{Sb} \\ &+ \frac{1}{A} \cdot n_{Fe} \cdot \bar{V}_{Fe} \\ &= d_0 + \frac{1}{A} \cdot n_{Fe} \cdot \bar{V}_{Fe} \end{aligned} \quad (4)$$

where n_i = amount of i,

\bar{V}_i = molar volume of i,

A = cross section of specimen.

Considering

$$n_i = \frac{m_i}{M_i}, \rho_i = \frac{M_i}{\bar{V}_i}, c_i = \frac{m_i}{V}$$

where m_i = mass of i,

M_i = molar mass of i,

ρ_i = density of i,

c_i = concentration of i,

V = total volume,

is received

$$d_{liq.} = d_0 \cdot \left(1 + \frac{c_{Fe(liq.)} \cdot \rho_{Sb}}{c_{Sb(liq.)} \cdot \rho_{Fe}} \right) \quad (5)$$

The concentration distribution of antimony out of the liquid mixed phase into iron is characterized by dissolving the diffusion equation (Equation 3). Solutions therefore are given standard work, like

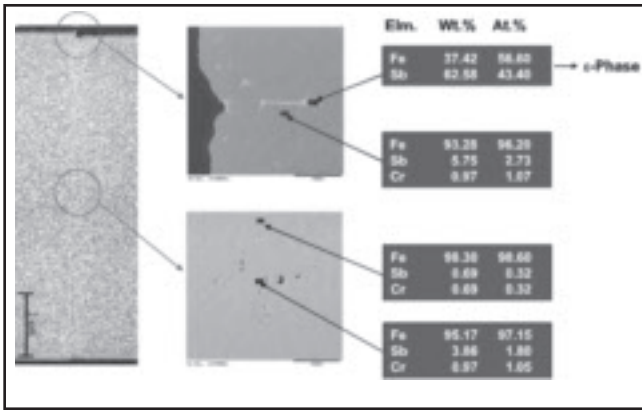


Fig. 4 — Micrographs, SEM pictures, and EDX-analysis of brazed steel specimens.

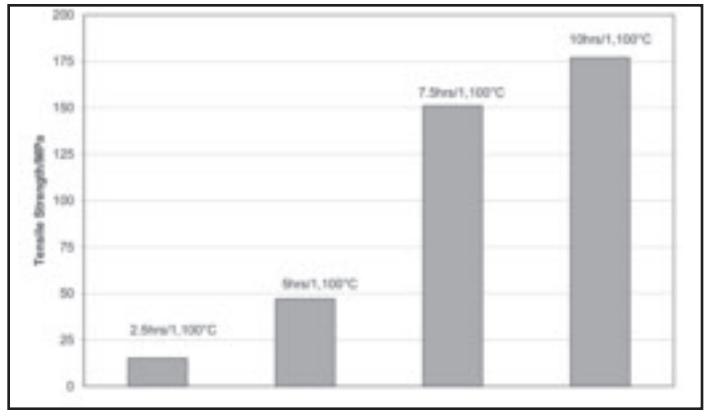


Fig. 6 — Tensile strength of brazed Fe samples as a function of exposure time to Sb gas.

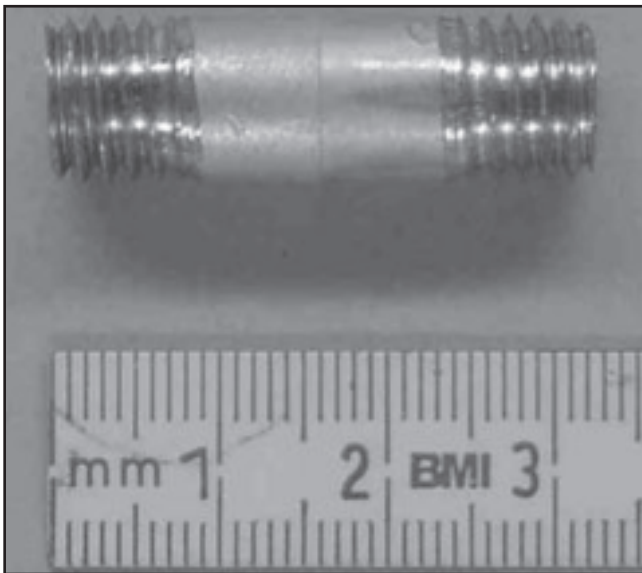


Fig. 5 — Sb-gaseous brazed Fe tensile test specimen.

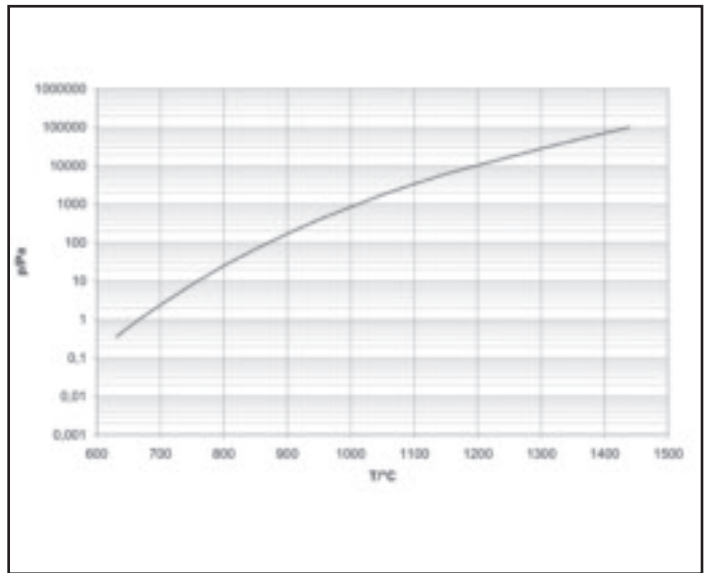


Fig. 7 — Antimony vapor pressure curve.

Ref. 16. The following terms are applied

$$\frac{\partial c_{Sb}}{\partial x} \Big|_{x=0} = 0; c_{Sb} = c_{Sb}^0 \text{ for } |x| > \left| \frac{d_{liq.}}{2} \right| \text{ and } t = 0$$

Equation 7 defines the Gaussian error function

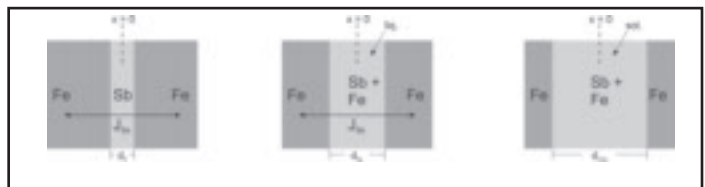


Fig. 8 — Braze experiment sequences.

As a result the antimony concentration distribution is given by

$$c_{Sb}(x,t) = \frac{1}{2} \cdot c_{Sb}(liq.) \cdot \left[\operatorname{erf} \left(\frac{\frac{d_{liq.}}{2} - x}{2 \cdot \sqrt{D_{Sb} \cdot t}} \right) + \operatorname{erf} \left(\frac{\frac{d_{liq.}}{2} + x}{2 \cdot \sqrt{D_{Sb} \cdot t}} \right) \right] \quad (6)$$

$$\operatorname{erf}(x) = \frac{2}{\sqrt{\pi}} \cdot \int_0^x e^{-x^2} dx \quad (7)$$

The experiments mentioned in the previous section are supported by Equation 6. With $D_{Sb} = 3 \cdot 10^{-9} \text{ cm}^2/\text{s}$ (according to Ref. 17) and $d_0 = 30 \mu\text{m}$ as well as $c_{Sb}(liq.) = 47 \text{ wt-}\%$ (Fig. 1), the concentration distribution depicted in Fig. 6 was the result. These calculations indicated that the equilibrium concentration was not yet reached

after 2.5 h and 5 h. Consequently, the formation of ϵ phase is impossible. With a duration of 7.5 h, the equilibrium concentration of α -Fe ($c_{Sb}(sol.) = 89.7 \text{ wt-}\%$) was achieved and the joint clearance was all but closed, which is in line with the experiments.

Conclusions

The presented method provides the opportunity of joining components with a gaseous phase by applying PVD-technol-

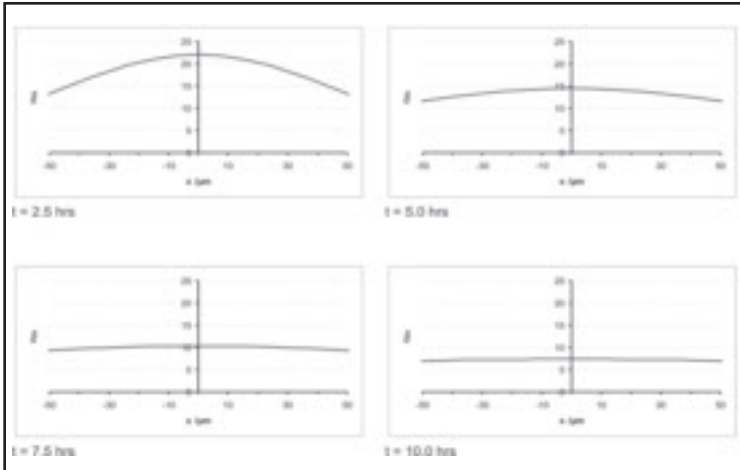


Fig. 9 — Concentration distribution of Sb calculated with Equation 6.

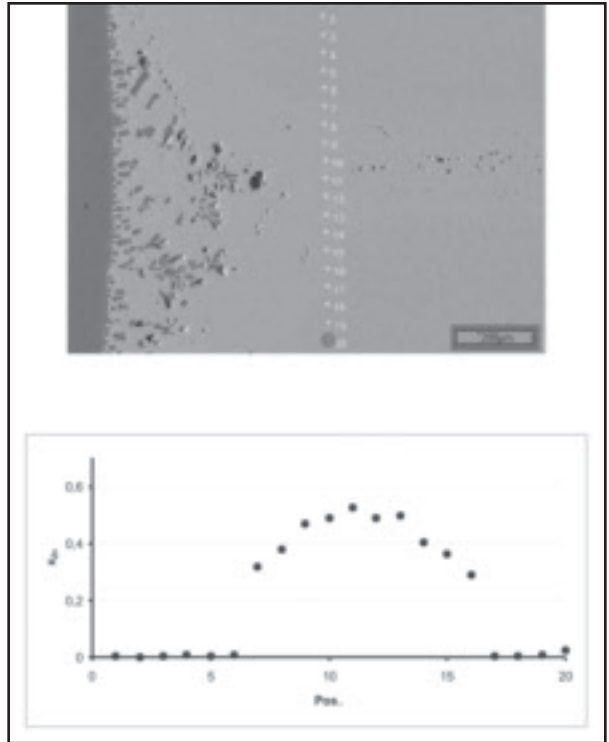


Fig. 10 — Nickel brazed with gaseous Zn (REM-photograph, concentration distribution).

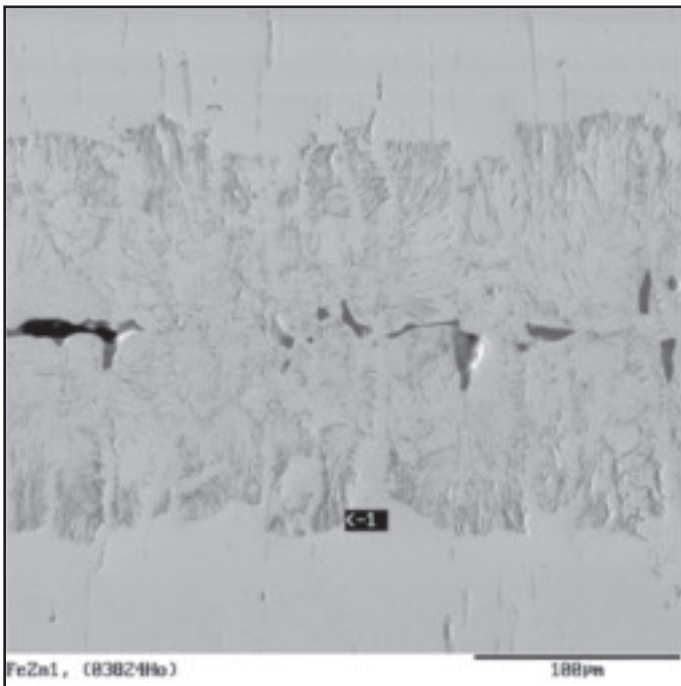


Fig. 11 — Iron brazed with gaseous Zn.

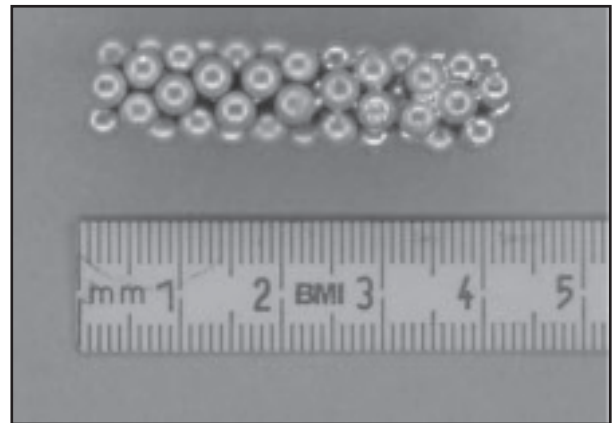


Fig. 12 — Rod of brazed steel balls using antimony gas.

ogy. Besides using antimony as a gaseous filler metal, other metals were considered. Brazing of nickel using zinc is also possible as seen in Fig. 7. Here within the brazing joint a β -phase (NiZn) can be found. In this system, the concentration distribution can be described qualitatively according to Equation 6 as well. The brazing of iron with gaseous zinc is also possible — Fig. 11.

This new joining technology is suitable for a series of applications. The gaseous braze transport allows small and complex components to be brazed where previ-

ously no joining technology was available. Potential applications can be found in microsystems or light construction. Goods in bulk, such as small steel balls, can be joined (Fig. 12), which offers the possibility of manufacturing low-weight rigid parts of any geometry.

References

1. Petrunin, I. E. 1991. *Handbuch Löttechnik*, 1st edition, Berlin, Verlag Technik.
2. *Brazing Handbook*, 4th edition, 1991. Miami, Fla.: American Welding Society.
3. Wielage, B., Hartung, F., Möhwald, K., and Ashoff, D. 1992. Löten Arc-PVD-metallisierter Ingenieurkeramik als Hybridtechnologie von Metall/Keramik-Verbindungen. *Fortschritt-Berichte VDI* 254(5): 16–31.
4. Steffens, H.-D., Hartung, F., and Möhwald, K. 1992. Metallisieren und Löten von Ingenieurkeramik als Hybridtechnologie für neue Einsatzgebiete. *DVS-Berichte* 148: 233 to 238.
5. Steffens, H.-D., Ashoff, D., Möhwald, K., and Müller, J.-U. 1994. Entwicklungen zum Löten von Keramik und Metall. *Fortschritt-Berichte VDI* 317(2): 40–54.
6. Steffens, H.-D., Wilden, J., and Möhwald,

K. 1995. Einsatz von Ionenplattierten Diffusionsbarrieren und Belotungssystemen beim Löten von Stahl/Leichtmetallverbindungen. *DVS-Berichte* 166: 94–98.

7. Steffens, H.-D., and Möhwald, K. 1997. Entwicklungstendenzen beim Löten unter dem Einsatz von Beschichtungen. *Fortschritt-Berichte VDI* 414(2): 107–121.

8. Möhwald, K. 1996. Einsatz des Ionenplattierens beim Löten. Ph. D. dissertation. University of Dortmund, Germany.

9. Bach, Fr.-W., and Möhwald, K. 1999. Einsatz metallischer Überzüge für neue Lösungswege in der Löttechnologie. *Info-Service Fachgesellschaft Löten* 1: 5–6.

10. Lugscheider, E., Bobzin, K., and Lake, M. K. 2001. Deposition of solder for micro-joining on M.E.M.S. components by means of magnetron sputtering. *Surface and Coatings Technology* 142: 813–816.

11. Sinclair, C. W., Purdy, G. R., and Morral, J. E. 2000. Transient liquid-phase bonding in two-phase ternary systems. *Metallurgical and*

Materials Transactions A 31A(4): 1187–1192.

12. Gale, W. F. 1999. Applying TLP bonding to the joining of structural intermetallic compounds. *The Journal of the Minerals, Metals and Materials Society* 51(2): 49–52.

13. Meyer, R. J., Peters, F., Gmelin, L., and Pietsch, L. H. E. 1952. Gmelins Handbuch der Anorganischen Chemie 18b. 68, Clausthal-Zellerfeld, Gmelin Verlag.

14. Zhou, Y. 2001. Analytical modeling of isothermal solidification during transient liquid phase (TLP) bonding. *Journal of Material Science Letters* 20(9): 841–844.

15. Cain, S. R., Wilox, J. R., and Venkatraman, R. 1997. A diffusional model for transient liquid phase bonding. *Acta mater.* 45(2): 701–707.

16. Crank, J. 1956. *The Mathematics of Diffusion*. England, Oxford Press.

17. Bruggeman, G. A., and Roberts Jr., J. A. 1975. The Diffusion of Antimony in Alpha Iron. *Metallurgical Transactions A* 6A: 755–760.

18. Müller, W., and Müller, J.-U. 1995. *Löt-*

technik: Leitfaden für die Praxis, Düsseldorf, Deutscher Verlag für Schweißtechnik DVS-Verlag GmbH.

Preparation of Manuscripts for Submission to the *Welding Journal* Research Supplement

All authors should address themselves to the following questions when writing papers for submission to the *Welding Research Supplement*:

- ◆ Why was the work done?
- ◆ What was done?
- ◆ What was found?
- ◆ What is the significance of your results?
- ◆ What are your most important conclusions?

With those questions in mind, most authors can logically organize their material along the following lines, using suitable headings and subheadings to divide the paper.

1) **Abstract.** A concise summary of the major elements of the presentation, not exceeding 200 words, to help the reader decide if the information is for him or her.

2) **Introduction.** A short statement giving relevant background, purpose, and scope to help orient the reader. Do not duplicate the abstract.

3) **Experimental Procedure, Materials, Equipment.**

4) **Results, Discussion.** The facts or data obtained and their evaluation.

5) **Conclusion.** An evaluation and interpretation of your results. Most often, this is what the readers remember.

6) **Acknowledgment, References, and Appendix.**

Keep in mind that proper use of terms, abbreviations, and symbols are important considerations in processing a manuscript for publication. For welding terminology, the *Welding Journal* adheres to AWS A3.0:2001, *Standard Welding Terms and Definitions*.

Papers submitted for consideration in the *Welding Research Supplement* are required to undergo Peer Review before acceptance for publication. Submit an original and one copy (double-spaced, with 1-in. margins on 8½ x 11-in. or A4 paper) of the manuscript. A manuscript submission form should accompany the manuscript.

Tables and figures should be separate from the manuscript copy and only high-quality figures will be published. Figures should be original line art or glossy photos. Special instructions are required if figures are submitted by electronic means. To receive complete instructions and the manuscript submission form, please contact the Peer Review Coordinator, Erin Adams, at (305) 443-9353, ext. 275; FAX 305-443-7404; or write to the American Welding Society, 550 NW LeJeune Rd., Miami, FL 33126.